Structural investigation of steel fibre reinforced concrete

R. BABUT
Institute of Fundamental Technological Research
of the Polish Academy of Sciences, Warsaw

1 Introduction

Steel fibres are used in concrete to create new structural materials which exhibit different mechanical properties as compared with the plain concrete matrix.

In spite of a large number of investigations, the design of mechanical properties and loadbearing capacities of SFRC elements is still an open problem.

In the case of steel fibre reinforced concrete, the materials specification will contain an additional number of variable parameters as compared with conventionally reinforced concrete, all strongly influencing the mean and the scatter of the mechanical properties.

Table 1. Characteristics of steel reinforced concrete.

		reinforcement	
type of concrete	diameter	effective content	effective distribution
conventionally	>8 mm	known	known
reinforced ferro-cement	1–2 mm	known	known
fibre reinforced	<0.8 mm	variable	variable

Factors influencing the fibre efficiency can be divided into two groups. The first contains factors which lead to an increase of the fibre efficiency by improvement of the bond properties of a single fibre (e.g. chemical or mechanical treatment of the fibre surface, irregular shape or mechanical anchorages at the ends of a fibre) as compared with the efficiency of the round straight fibre. The second relates to the fibre structure: inhomogeneity of the fibre distribution along an element, segregation of fibres over the depth of an element and effectiveness of the fibre orientation. These three factors may reduce the strength of steel fibre reinforced concrete in relation to the strength of an hypothetical composite material in which fibres should be uniformly distributed and aligned in the direction of the principal tensile stress in an element.

Extensive systematic investigations of factors in the first-mentioned group have been carried out. On the other hand, the factors of the second group are dealt with in only a small number of publications [1–5], insufficient for general conclusions for design purposes. A theoretical background and practical methods for the analysis have been given by, among others, Kasperkiewicz [6] and Stroeven [7, 8].

A comprehensive experimental programme for investigating the structure of reinforcement in various SFR concretes has been carried out at the Delft University of

Technology*. The paper focuses on the methodology of structural analysis applied and on parameters that could characterize the effective structure of fibrous reinforcement. Variations in the structure of the investigated composites have been compared into variations in mechanical properties determined in a tensile mode. The later aspect of the investigation will be reported elsewhere.

2 Scope of the investigation

The main purpose of the investigation was an examination of factors that influence the internal structure of the steel fibre reinforcement: the fibre distribution, the effective fibre content and the fibre orientation are to be regarded as important design parameters. Their quantitative determination would yield systematic data necessary for the design of SFRC elements. All these factors directly depend on the properties of the fresh concrete matrix and the process of preparation of specimens and elements.

The following material and technological parameters were varied: vibration time, matrix workability (both technological parameters) and fibre content (material parameters). The block diagram of the investigations is presented in Fig. 1.

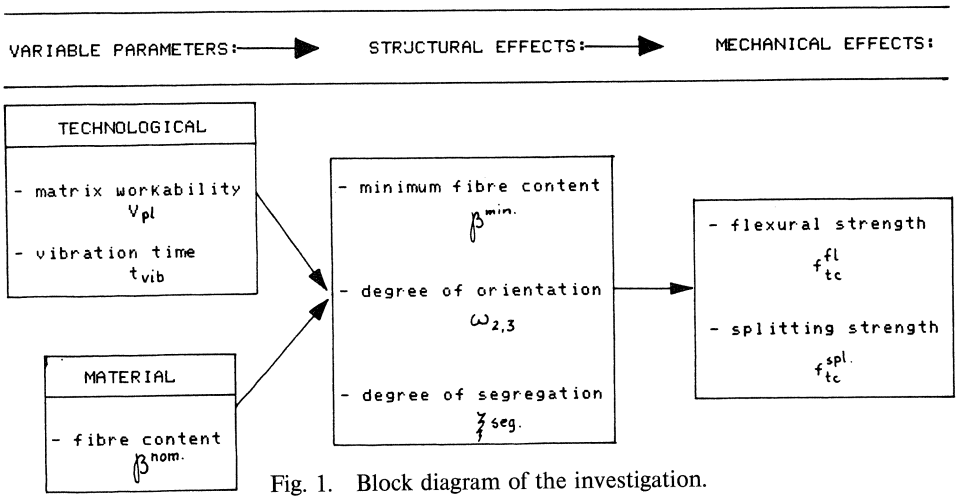

Fig. 1. Block diagram of the investigation.

Main aims of the research were the determination of:

i. the minimum fibre content in the tested elements;
ii. the influence of the technological and materials variables on distribution, segregation and orientation of the fibres;
iii. the relations between parameters describing effective fibre structures of the reinforcement and the mechanical properties of SFR concretes.

* Joint investigation by the Group of Material Sciences of the Department of Civil Engineering (DUT, Delft) and the Group of Strain Fields (IFTR, Warsaw).

3 Details of SFRC mixes and specimens

A plain concrete with a maximum aggregate size of 8 mm, a w/c ratio of 0.5 and a portland cement content of 375 kg/m^3 served as the reference material.

The straight fibres of ARBED type with diameter of 0.38 mm and length of 25 mm were used throughout the experiments.

As a result, common method for improving the mechanical behaviour of SFRC may be provided with a structural basis. To that end, answer has to be given to the question which parameters should be introduced into the designer's calculations.

Three series of steel fibre reinforced concretes were prepared, with the variable parameters specified as follows:

Series I - nominal fibre content β^{nom} (% by volume) - mixes P1, P2, P3, P10, P11, P12;
Series II - amount of superplasticizer, V_{pl}(% by weight of cement) - mixes P3, P4, P5, P6;
Series III - vibration time, t_{vib} - mixes P6, P7, P8, P9.

The specification of all the mixes is given in Table 2.

Twelve steel fibre reinforced concrete slabs with dimensions of 700 mm × 500 mm × 100 mm (width × length × thickness) were cast. They are denoted by P1, P2, ..., P12 according to Table 2. The moulds were filled directly from the mixer to avoid

Table 2. Specification of plain concrete and SFRC mixes.

		fibre content β^{nom}, (% by volume)						
		0.0	0.5	1.0	1.5	2.0	2.5	3.0
content of superplasticizer, V_{pl} (%);	0.0	M120	P.1	P.2	P.3			
	0.7				P.4	P.10		
	1.4				P.5		P.11	
	2.0				P.6			P.12
($t_{vib} = 120$ sec)								
vibration time, t_{vib} (sec);	0	M 0			P.7			
	60	M 60			P.8			
	120	M120			P.6			
	180	M180			P.9			
($V_{pl} = 1.5\%$)								

adverse effects during the casting with separate portions. The slabs were compacted on the vibrating table.

For the purpose of mechanical tests each slab was cut into six prisms with dimensions of 100 mm × 100 mm × 500 mm. After the prisms had been tested in bending, two 100 mm cubes were cut for the splitting tensile test. Testing methods and results of the mechanical test are described in [9].

4 Method of analysis for the structure of SFR concretes

4.1 *Method of analysis*

Stereological image analysis techniques were used in this investigation for determining the spatial arrangement of the fibres. Fibre content and fibre distributions were determined by counting fibre intersections visible in chosen cross-sections in the elements.

A QUANTIMET 720 (quantitative image analyser) connected to a PDP-11 computer was used for the automatic morphometric analysis. Since it was not possible to observe the ground surface of the fibre concrete directly by the T.V. camera of the analyser (the number of recorded fibre intersections varied with the angle of observation and with the intensity of the light), the fibre patterns were prepared by copying the fibre positions on transparent sheets. About 300 patterns were analysed in this investigation. An example of a fibre pattern is shown in Fig. 2.

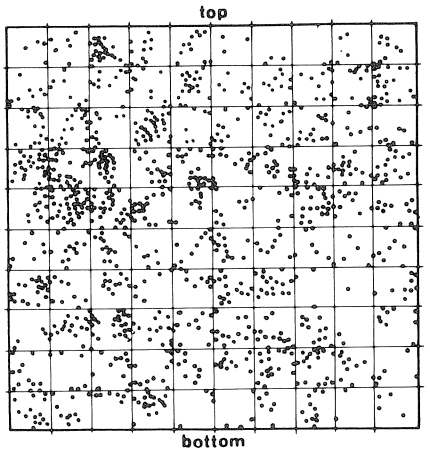

Fig. 2. Manually copied fibre pattern of a cross-section from slab P12, $\beta^{nom} = 3.0\%$.

4.2 *Sampling of SFRC specimens*

For the purpose of the morphological analysis the first saw cuts were made as near as possible to the cross-section at which the failure occurred, in flexural or in splitting tests. Additionally, one cross-section at the lateral face of each prism was randomly selected for the analysis. The cross-sectional dimensions were about 100 mm × 100 mm. At least 24 cross-sections from each slab were analysed: 18 for the direction parallel to the direction of vibration and 6 for the perpendicular direction. The distribution of the analysed cross-sections in a single prism is shown in Fig. 3. A full set of diagrams representing the distributions of the cross-sections is given in [10].

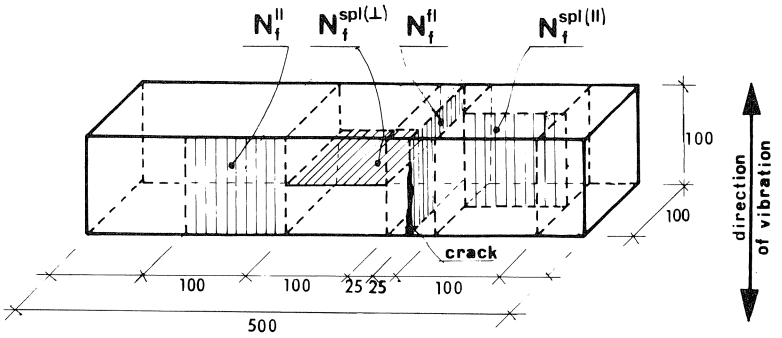

Fig. 3. Distribution of the cross-sections considered in the stereological analysis in a prism 100 mm × 100 mm × 500 mm.

4.3 *Computer procedure in the stereological analysis*

Two computer programs were prepared for the investigation*. The first program was used for analysing the recorded images of the fibre patterns. First, blocks and chains of points were split into single features. The total number of these features was then displayed. The X, Y coordinates of all the features were finally recorded in the disk memory (i.e. this is basically an erosion operation in image processing).

The second program served to divide the analysed image into ten horizontal and vertical strips, all about 10 mm in width. Next, the number of features in each strip was calculated. Examples of the computer printouts are shown in Fig. 4. The following image analysis data are given:

- identification number of image (cross-section);

```
INPUT DATA FILE NAAM (MAX 6 TEKENS) ?P12X63
LEFT = .446903 MM        RIGTH = 106.214 MM
NUMBER = 1174     AREA = 10080.6 MM2     N/A = .116461 MM-2   Nf

| A | AREA 10080.6 |   | NUMBER 1174 | N |   | MEAN 47.248 | ȳ | STAND.DEV 28.3191 |   | VAR.COEF .599372 |

DISTANCE    NUM  ....1....2....3....4....5....6....7....8....9....10=250
  5.05      100  ********************
 15.15      151  ******************************
 25.25      162  ********************************
 35.35      134  ***************************
 45.45      107  *********************
 55.55      114  ***********************
 65.65      107  *********************
 75.75      114  ***********************
 85.85       75  ***************
 95.95      110  **********************
```

Fig. 4. Computer printout in the form of a histogram of the fibre intersections in horizontal or vertical strips.

* The author deeply appreciates the help he received from Ir. J. Luijerink and C. van Dam adjusting the QUANTIMET 720 analyser and preparing the computer programs.

- total number of features counted and recorded;
- area of the fibre pattern;
- average number of fibre intersections per mm^2;
- mean values of X- and Y-coordinates (coordinates of the centre of gravity of the micro reinforcement);
- distances (in mm) of centre lines of the strips from the zero position;
- number of fibres in each horizontal and vertical strip and their graphical presentation.

4.4 *Minimum pattern size for the stereological analysis*

To achieve good representativeness of the stereological analysis, short tests were executed to examine the influence of the size of a fibre pattern on the variation of the readings.

Coaxial square areas with dimensions of 10 mm × 10 mm, 50 mm × 50 mm, 75 mm × 75 mm and 100 mm × 100 mm on the selected fibre patterns of series I were analysed. The numbers of fibre intersections were recorded. Results obtained (N_f^{ef} = effective number of fibre intersections) are compared in Fig. 5 with expected values determined for the

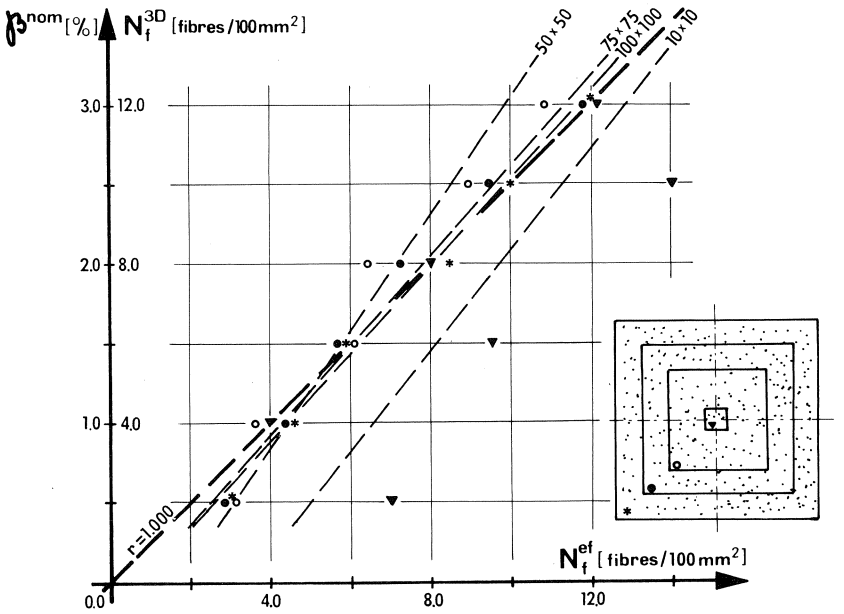

Fig. 5. Comparison of the effective N_f^{ef} and expected N_f^{3D} numbers of fibre intersections determined in the coaxial areas: 10 mm × 10 mm, 50 mm × 50 mm, 75 mm × 75 mm and 100 mm × 100 mm. Right, the arrangement of the analysed areas.

nominal fibre content, N_f^{3D}. Values of N_f^{3D} were calculated from a formula given by Kasperkiewicz [6]:

$$N_f^{3D} = \frac{\pi \cdot d^2}{2 \cdot \beta^{nom}} \cdot 100, \text{ fibres/100 mm}^2 \quad (1)$$

where:

d = diameter of fibre, in mm
β^{nom} = nominal fibre content, per cent by volume
π = 3.14

Theoretical and experimental data for each size of area are compared. To that end, linear regression lines have been plotted in Fig. 5. It can be concluded that areas of 75 mm × 75 mm and 100 mm × 100 mm are large enough to achieve sufficient accuracy of the calculations, since the regression lines for the experiments are situated close to the theoretical line.

In all the investigations, samples approximately 100 mm × 100 mm in size were used.

5 Parameters of the fibre structure

5.1 *Effective fibre content*

The fibre content was determined in the cross-sections parallel to and perpendicular to the direction of action of the vibrating forces during the compaction of elements on the table as shown in Fig. 3. These directions are designated by ∥ and ⊥, respectively.

The detailed numerical results of the stereological analysis of the effective fibre content for all series are presented in Table 3, which allows comparison of the overall number of fibre intersections $\bar{N}_f^{\parallel}$ (mean value of 18 readings, minimum), the number of fibre intersections in cross-section failed in flexure $\bar{N}_f^{fl}$ and in splitting tension $\bar{N}_f^{spl(\parallel)}$ (both, mean values of 6 readings); also the lowest observed values of $\check{N}_f^{\parallel}$ as compared with the nominal (expected) values N_f^{3D} calculated from formulae (1) for an ideal 3-dimensional fibre structure (the superscript 3D is used throughout the text for all these values).

The corresponding values of the standard deviation (s.d.) and of the coefficient of variation (c.v.) are also given.

The data presented in Table 3 were used to determine other parameters that could be used in the description of the effective structure of reinforcement in SFRC elements.

5.2 *Minimum fibre content*

With respect to the mechanical properties of steel fibre reinforced concretes the minimum fibre content may have a meaning similar to that of the minimum strength of plain concretes. From the results of Series I the lowest values of $N_f^{\parallel}$ were selected to define the possible minimum of the number of fibres per unit area $\check{N}_f^{\parallel}$. These results of the

Table 3. Results of the stereological analysis of the effective fibre contents.

slab no.	nominal fibre content β^{nom} %	content of super-plasticizer V_{pl} %	vibration time t_{vib} sec.	(nom.) number of fibres effective (parallel direction) $\bar{N}_f^{3D}$ fibres/100 mm²	$\bar{N}_f^{\parallel}$ fibres/100 mm²	s.d.	c.v. %	$\bar{N}_f^{fl}$ fibres/100 mm²	s.d.	c.v. %	$\bar{N}_f^{spl(\parallel)}$ fibres/100 mm²	s.d.	c.v. %	number of fibres effective (perpendicular dir.) $\bar{N}_f^{spl(\perp)}$ fibres/100 mm²	s.d.	c.v. %	numb. of fibres minimum $\check{N}_f^{\parallel}$ fibres/100 mm²	$\check{N}_f^{\perp}$ fibres/100 mm²
SERIES I																		
P1	0.5	0.0	120	2.0	2.38	±0.47	19.7	2.34	±0.41	17.5	2.36	±0.48	20.3	1.87	±0.47	25.1	1.62	1.31
P2	1.0	0.0	120	4.0	4.53	±0.90	19.8	3.98	±0.49	12.3	4.59	±1.02	22.2	4.12	±0.92	22.3	3.11	3.08
P3	1.5	0.0	120	6.0	6.26	±0.94	15.0	6.08	±0.49	8.0	6.11	±0.99	16.2	4.22	±0.62	14.7	4.68	3.62
P10	2.0	0.7	120	8.0	9.22	±1.36	14.8	8.74	±0.64	7.3	8.94	±1.47	16.4	4.63	±1.03	22.7	6.36	3.64
P11	2.5	1.4	120	10.0	10.48	±1.54	14.4	10.32	±1.73	16.7	11.11	±1.87	15.9	6.60	±1.85	28.0	7.54	3.41
P12	3.0	2.0	120	12.0	13.00	±1.89	14.6	12.69	±1.66	13.1	12.29	±1.30	10.6	4.12	±1.08	26.2	10.00	3.23
SERIES II																		
P3	1.5	0.0	120	6.0	6.26	±0.94	15.0	6.08	±0.49	8.0	6.11	±0.99	16.2	4.22	±0.62	14.7	4.68	3.62
P4	1.5	0.7	120	6.0	6.31	±1.15	18.2	5.75	±0.82	14.3	6.77	±1.55	22.9	5.07	±0.85	16.8	4.82	3.64
P5	1.5	1.4	120	6.0	6.63	±0.98	15.4	6.68	±0.82	12.3	6.83	±0.87	12.7	4.48	±0.79	17.6	4.37	3.64
P6	1.5	2.0	120	6.0	6.15	±1.09	17.7	6.47	±1.24	19.2	5.57	±0.89	16.0	3.84	±0.83	21.6	4.36	2.73
SERIES III																		
P7	1.5	2.0	0	6.0	6.20	±1.34	21.6	7.41	±0.62	8.4	6.08	±0.40	6.6	2.01	±0.90	44.8	3.34	1.03
P8	1.5	2.0	60	6.0	6.41	±1.32	20.6	6.84	±0.83	12.1	6.07	±0.61	9.9	3.25	±0.64	20.1	3.64	1.92
P6	1.5	2.0	120	6.0	6.15	±1.09	17.7	6.47	±1.24	19.2	5.57	±0.89	16.0	3.84	±0.83	21.6	4.36	2.73
P9	1.5	2.0	180	6.0	6.43	±1.24	19.3	6.92	±0.91	13.1	6.02	±1.26	20.9	3.74	±1.19	31.8	4.12	2.29

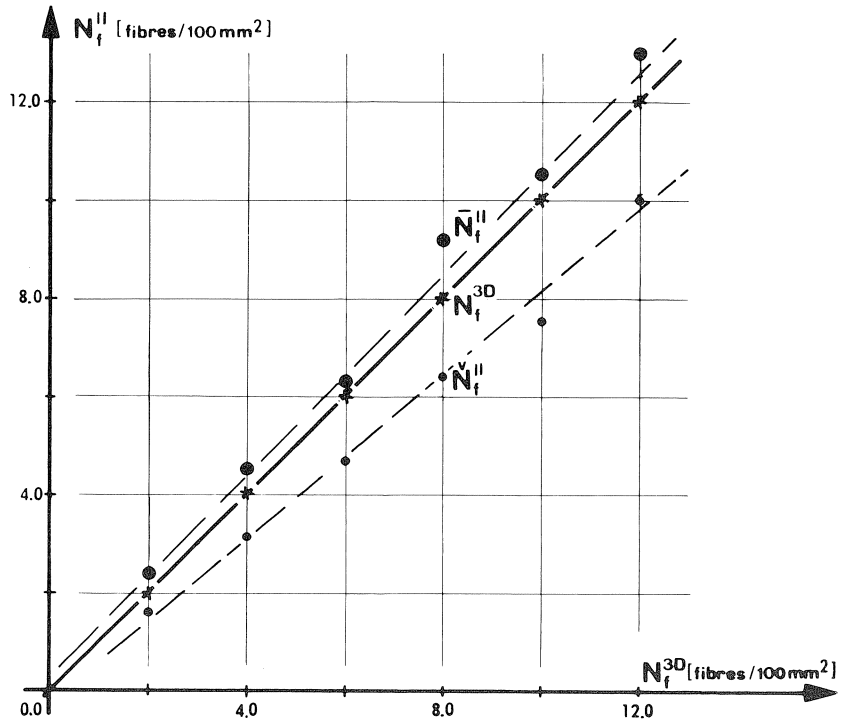

Fig. 6. Lowest observed number of intersections per unit area $\check{N}_f^{II}$ as a function of the expected values N_f^{3D} in the slabs of Series I. $\bar{N}_f^{II}$ = mean value in slab.

QUANTIMET readings are shown in Fig. 6 as a function of the expected values.

The scatter in the results can be defined by means of the coefficient of variation. Such values were calculated from at least 18 readings. Alternatively, scatter was revealed by the coefficient γ which expresses the relative distance of the minimum value $\check{N}_f^{II}$ from the expected value N_f^{3D} and, in fact, an effective reduction of the fibre content. γ is calculated from:

$$\gamma = \frac{N_f^{3D} - \check{N}_f^{II}}{N_f^{3D}} \tag{2}$$

The variation in the values of γ in all the series is presented in Table 4.

5.3 *Degree of orientation of the fibre structure*

The orientation distribution of fibres for all the series was determined on the basis of the average values per slab for the effective fibre content in perpendicular and parallel cross-sections. The degree of orientation of the fibre structure can be determined by the formulae given by Stroeven in [8]. Assuming that fibres have a spatial orientation which can be classified between two ideal situations, namely between 3-dimensional (3D) and

2-dimensional (2D) orientation, the expression for the degree of orientation has the form:

$$\omega_{2,3} = \frac{N_f^{\parallel} - N_f^{\perp}}{N_f^{\parallel} + 0.273 \cdot N_f^{\perp}} \tag{3}$$

where $N_f^{\parallel}$ and $N_f^{\perp}$ are the effective numbers of fibre intersections per unit area determined for two orthogonal planes: here, parallel and perpendicular to the direction of the vibrating forces. For an ideal 3-dimensional fibre orientation the value of ω_3 is 0.0. This means that fibres are oriented with equal probability in all spatial directions. In the case of fully planar alignment of fibres the value of ω_2 is 1.0.

The influence of material composition and of technological parameters - used to differentiate between the steel fibre reinforced concretes investigated - on the degree of orientation of the fibre structure is shown in Table 4.

Table 4. Effective values of the stereological parameters of the structure of steel fibre reinforcement.

slab no.	nominal fibre content β^{nom} %	content of super-plasticizer V_{pl} %	vibration time t_{vib} sec	degree of reinforcement reduction γ -	degree of orientation $\omega_{2,3}$ -	degree of segregation ξ_{seg} -
SERIES I						
P1	0.5	0.0	120	0.19	0.171	0.56
P2	1.0	0.0	120	0.22	0.082	0.57
P3	1.5	0.0	120	0.22	0.260	0.54
P10	2.0	0.7	120	0.20	0.422	0.52
P11	2.5	1.4	120	0.24	0.351	0.55
P12	3.0	2.0	120	0.16	0.609	0.50
SERIES II						
P3	1.5	0.0	120	0.22	0.260	0.54
P4	1.5	0.7	120	0.19	0.208	0.53
P5	1.5	1.4	120	0.27	0.292	0.54
P6	1.5	2.0	120	0.24	0.261	0.53
SERIES III						
P7	1.5	2.0	0	0.44	0.614	0.50
P8	1.5	2.0	60	0.39	0.405	0.53
P6	1.5	2.0	120	0.24	0.261	0.53
P9	1.5	2.0	180	0.31	0.320	0.55

5.4 *Segregation of the fibres*

There exists no particular rule as to how segregation of fibres should be measured. A very simple method was used in [11], in which the fibre contents in the upper and lower halves of analysed cross-sections were compared. In the reported investigation another possibility was opened, since the X- and Y-coordinates of all the fibre intersections in

the image plane were recorded by means of the QUANTIMET 720 analyser and associated computer.

The coefficient ξ_{seg} was introduced as the indicator of the degree of segregation:

$$\xi_{seg} = \bar{y}/h \tag{4}$$

where:

$\bar{y}$ = coordinate of the centre of gravity of the reinforcement
h = height (or depth) of the analysed cross-section parallel to the direction of vibration

The position of the centre of gravity of the reinforcement was calculated as the average value of the coordinates of all the recorded fibre intersections in an analysed cross-section. Hence, the size differences of the intersections were not considered. In the case of an ideal fibre distribution the value of ξ_{seg} would be 0.5.

The results of the analysis of the degree of segregation are given in Table 4. At least 18 cross-sections were analysed per slab.

An alternative method of analysis of the distribution of fibres over cross-sections has been discussed in [12].

6 Discussion of the results

The effective fibre content can be studied from the results in Table 3. On the average, the effective fibre contents in planes parallel to the direction of vibration in all the series are about 2–19% higher than the expected values N_f^{3D}. This can be explained by the degree of orientation of the fibres due to a partially-planar structure of the reinforcement. An increase in the number of fibre intersections in parallel planes coincides with a decrease in perpendicular planes. Decrease is, however, more dramatic. This can be quantitatively explained. The transformation of a portion of the 3-D distributed fibres to a planar system somewhat increases the number of intersections in a plane perpendicular to the orientation plane of the fibres (efficiency increases from 1/2 to $2/\pi$), but reduces this number in a parallel plane (efficiency reduction from 1/2 to 0). This effect is more pronounced for higher volume fractions of fibres, since the planar oriented portion increases with the volume fraction and is reflected in the approximately linear increase of ω with β^{nom}, $r = 0.875$.

In Fig. 7 the results of the QUANTIMET readings are presented for all cross-sections of Series I, comprising a full range of fibre contents. The value of N_f represents the number of fibre intersections per unit area (10 mm × 10 mm = 100 mm^2). The results for parallel planes seem to fit best to a straight line. A linear regression analysis yields a correlation coefficient $r = 0.950$. The curvilinear regression applied to the results for perpendicular planes yields the parabola $F(x) = -0.34 + 1.28x - 0.07x^2$ ($r = 0.856$).

The continuous line in the diagram represents the line of ideal agreement ($r = 1.00$) of experimental and theoretical values.

The scatter of fibre content in parallel planes seems to be independent of the param-

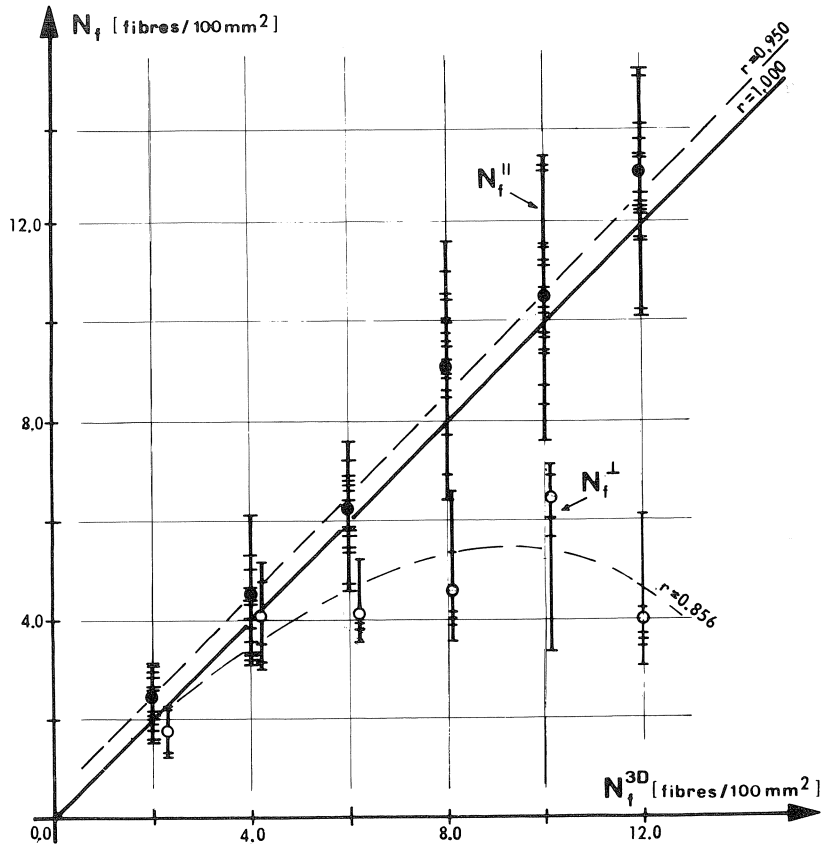

Fig. 7. Effective fibre contents $N_f^{\parallel}$ and $N_f^{\perp}$ in cross-sections parallel and perpendicular, respectively, to the direction of vibration as functions of the predicted fibre intersections N_f^{3D} per unit area. The points represent the group averages.

eters introduced in the investigation, although addition of superplasticizer seems to reduce the scatter slightly.

The lowest observed number of fibre intersections $\check{N}_f^{\parallel}$ was compared with the predicted theoretical values of N_f^{3D}. Special attention was given to Series I. It could be expected that for low fibre contents the value of γ (coefficient which determines the relative distance of the minimum value from the expected average value) should be significantly higher, since there is more possibility for non-uniform fibre distribution as compared with series containing high fibre contents. This supposition is not confirmed. The values of γ vary from 0.16 to 0.24. The number of 18 analysed cross-sections per plate was too small for a thorough statistical analysis. Hence, only a simplified analysis can be applied using the standard deviation to define the characteristics (i.e. minimum) value of the fibre content.

In the case of N_f^{3D} a value of 20.0% for the coefficient of variation can be assumed for further analysis. In this investigation, coefficients of variation of about 20% were

obtained. They are relatively small in relation to the values of about 70% previously obtained by the present author [13]. According to the assumption, the value for the standard deviation calculated in this analysis is $0.2 \cdot N_f^{3D}$. Assuming a 10% level of significance, the limit range for the number of fibre intersections in the case of 18 readings is determined as follows:

$$N_f^{3D} - 1.74\ s.d. < N_f < N_f^{3D} + 1.74\ \text{s.d.}$$

The results of the analysis of the limit ranges for Series I are presented in Table 5. Not a single value of N from Series I fell below the lower limit.

Table 5. Comparison of the calculated lower and upper limit values of N_f^{3D} with the observed average, maximum and minimum values.

	number of fibre intersections N_f, fibres/100 mm^2					
slab no.	nominal value N_f^{3D}	actual average $\bar{N}_f^{\parallel}$	calculated lower limit N_f^L	observed minimum value $\tilde{N}_f^{\parallel}$	calculated upper limit N_f^U	observed maximum value $\hat{N}_f^{\parallel}$
P1	2.0	2.38	1.36	1.62 (0)*	2.63	3.11 (4)*
P2	4.0	4.53	2.70	3.11 (0)	5.30	6.09 (3)
P3	6.0	6.26	3.96	4.68 (0)	8.04	7.86 (0)
P10	8.0	9.22	5.42	6.36 (0)	10.58	11.62 (1)
P11	10.0	10.48	6.60	7.54 (0)	11.40	13.37 (3)
P12	12.0	13.00	8.00	10.00 (0)	16.00	15.12 (0)

* In parentheses the number of observations outside the region between lower or upper limits; total number of observations per line is 18.

The observed actual averages $\bar{N}_f^{\parallel}$ of all the composites were higher than the nominal values. Hence, it could be concluded that the effective fibre contents move towards safer regions, provided that the loaded cross-section is favourably oriented in relation to the direction of gravity.

The discussion of the stereological parameters that characterize the structure of the fibrous reinforcement is based on the numerical results presented in Table 4.

The degree of orientation of reinforcement structures can be studied on Series I, since significant differences in the values of ω were obtained. The results indicate a direct relation between the fibre content and the degree of orientation. With an increase in fibre content the structure of reinforcement became more planar.

The superplasticizer was used in the investigation to influence the mobility of the fibres during vibration. However, detected changes in the fibre orientation due to this factor were rather small. Increasing the vibration time from 0 sec to 120 sec led to results which were contrary to expectations. The fresh fibre concrete mix without vibration exhibited a more closely planar orientation than after vibration. That means that during compaction on the vibrating table the fibres tended to recover from the originally induced anisometry.

The degree of segregation of the fibres in the composites examined was too low for a

more elaborate analysis. The coefficient of variation of the ξ_{seg}-values within all the series was not more than 10%. With an increase of fibre content a slight decrease of ξ_{seg} can be observed. The very reason of this could be the stiff concrete matrix used. However, the admixture of superplasticizer in most of the mixes should stimulate the movement of fibres towards the bottom of the mould. On the other hand, the fibres are blocked by themselves and by the aggregate structure, and this may explain such behaviour of fibre reinforcement.

7 Conclusions

Stereological image analysis technique offers a tool for examining the effective structure of fibrous reinforcement and quantifying the parameters to be recommended for the design of steel fibre reinforced concretes.

Automation of the computing process can be effectively used in the analysis to reduce time-consuming operations.

The investigation proved that steel fibre reinforced concrete cannot be regarded as an isotropic material and that its actual structure cannot be ignored in investigations of this material.

The variations in the range of the parameters that occurred in the investigation were contrary to expectations. However, low amounts of scatter indicated good quality of the composite mixes used. Under different test or production conditions the scatter characterizing the actual structure is liable to be significantly greater.

Even small changes in the structure of fibre reinforcement can be expected to cause some improvement in mechanical properties. The possibility of better adjusting the fibres to the actual requirement, i.e. to the actual state of stress, without special treatment of the fresh mix and without extra cost, should also be regarded as an economic advantage.

Acknowledgements

The experimental program was carried out at the Delft University of Technology, under the Cultural Agreement between the governments of Poland and of the Netherlands. The author wishes to thank the Materials Science Group for the kindness he experienced during his stay at Delft and especially wishes to thank Mr. L. Donker for his technical assistance in carrying out the experiments.

References

1. Stroeven, P., Use of radiography-image analysis for steel fibre reinforced concretes. Proc. RILEM Symposium on: Testing and test methods of fibre cement composites - Sheffield, April 1978. The Construction Press Ltd, Lancaster 1978, pp. 275-288.
2. Malberg, B., Skarendahl, O., Kasperkiewicz, J., Determination of fibre content, distribution and orientation in steel fibre concrete by X-ray technique. As [1], pp. 297-305.
3. Babut, R., Effective distribution of dispersed fibres and its influence on mechanical properties of steel fibre reinforced concretes. Proc. Conf. on: Mechanics and technology of com-

posite materials - Varna, October 1982. Bulgarian Academy of Sciences, Sofia 1982, pp. 576–579.
4. Potrzebowski, J., The splitting test applied to steel fibre reinforced concrete. The Intern. Journal of Cement Composites and Lightweight Concrete, Vol. 5, No. 1, 1983, pp. 49–53.
5. Jamrozy, Z, Sliwinski, J., Structure of steel fibre reinforced concrete produced by rotational method, in Polish, Proc. 22nd Conf. PZITB, Krynica 1976.
6. Kasperkiewicz, J., Fibre spacing in steel fibre reinforced composites. Materiaux et Construction, Vol. 10, No. 55, 1977, pp. 25–31.
7. Stroeven, P., Morphometry of fibre reinforced cementitious materials. Part I: Efficiency and spacing in idealized structures. Materiaux et Constructions, Vol. 11, No. 61, 1978, pp. 31–38.
8. Stroeven, P., Morphometry of fibre reinforced cementitious materials. Part II: Inhomogeneity, segregation and anisometry of partially oriented fibre structure. Materiaux et Construction, Vol. 12, No. 67, 1979, pp. 9–20.
9. Babut, R., Structural and mechanical investigations of steel fibre reinforced concrete. Stevin Laboratory Report, Delft University of Technology, September 1985, 70 pp.
10. Donker, L., Mechanische eigenschappen van staalvezelbeton in afhankelijkheid van de verdeling van staalvezels in beton. Stevinrapport 1-83-18, Delft University of Technology, December 1983, 300 pp.
11. Babut, R., Effective structures of fibrous reinforcement and its influence on load-bearing capacity of SFRC elements in bending. In volume: Some aspects of mechanics of composite materials. Polytechnic of Bialystok, 1982, in Polish, pp. 171–212.
12. Stroeven, P., Babut, R., Wire distribution in steel wire reinforced concrete. Proc. The IV European Symposium for Stereology - Goteborg, August 1985.
13. Babut, R., Theoretical and experimental analysis of the load-bearing capacity of SFRC elements in bending. PhD Thesis, IFTR Warsaw, 1983.